

Research Article

Textile Multiantenna Technology and Relaying Architectures for Emergency Networks

Estefanía Crespo-Bardera ¹, Adrián Vega Delgado,¹ Aarón Garrido Martín,² Alfonso Fernández-Durán,² and Matilde Sánchez-Fernández¹

¹The Signal Theory & Communications Department, Universidad Carlos III de Madrid, Spain

²Nokia Spain, María Tubau 9, 28050 Madrid, Spain

Correspondence should be addressed to Estefanía Crespo-Bardera; ecrespo@tsc.uc3m.es

Received 2 November 2018; Accepted 22 January 2019; Published 5 February 2019

Guest Editor: Maurizio Casoni

Copyright © 2019 Estefanía Crespo-Bardera et al. This is an open access article distributed under the Creative Commons Attribution License, which permits unrestricted use, distribution, and reproduction in any medium, provided the original work is properly cited.

Every year around 200 million people are affected by hazards of different nature. In most of these situations public protection and disaster relief personnel are usually the first responders to provide help. To provide differential relief coverage in these scenarios, novel communication and network functionalities are being demanded, relegating today's narrowband private radio (PMR) emergency systems to the background. These are data-support, increased coverage, broadband communication, and high reliability which will be addressed by novel communication technologies such as Long Term Evolution (LTE), LTE Advanced-pro, and future 5G. In this work we tackle two key technological solutions for future emergency communication networks such as an architecture based on relay nodes and enhanced user equipment by means of multiple-input-multiple-output (MIMO) techniques.

1. Introduction

In the last decade, a total of 6,090 disasters were reported globally, originated from both natural hazards such as climatological, geophysical, meteorological, hydrological, and biological and artificial or technological hazards, being industrial, transport, and miscellaneous [1]. This figure yields around 600 disasters per year around the globe.

This amount of disasters has implied that 771,911 people were deceased under those circumstances over the last 10 years. In addition, the figure for the people affected by these hazards is close to 200 million every year, understanding people affected as those who were injured, whose house was destroyed, or those who required immediate help and aid such as salvage, basic survival needs, and medical aids [2].

Data on the number of people affected and the typology of the disaster are very useful information for disaster awareness, for the potential planning of a response and for the definition of future strategies for lowering disaster

impact. The reduction of disaster risk and disaster losses is the objective of the Sendai Framework for Disaster Risk Reduction (DRR) 2015–2030 [3], proposing a broad people-centered approach and a shift in emphasis from disaster management to disaster risk management. Many measures are to be tackled with this purpose: economic, structural, legal, social, health, cultural, educational, environmental, technological, political, and institutional. Nevertheless, even within this broad approach there is in most of the cases a first need for human intervention for emergency reaction after the disaster and this is where first responders, public protection, and disaster relief personnel or emergency services appear. Specifically, Priority 4 “Enhancing disaster preparedness for effective response and to *Build Back Better* in recovery, rehabilitation and reconstruction” [3] deals with, among others, contingency programs, resilience of infrastructure, workforce training, disaster risk, social technologies, hazard-monitoring telecommunications systems, and emergency communications infrastructure. Hence, technology and, in particular, communication and information systems are two

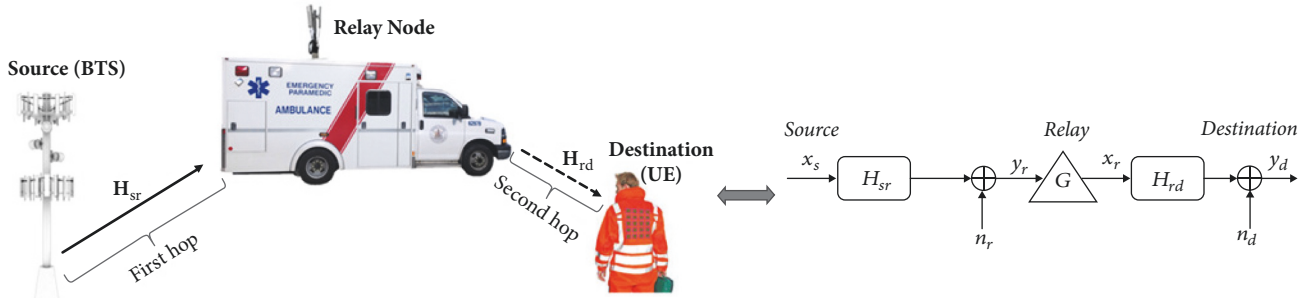


FIGURE 1: System model of a two-hop half-duplex single relay scenario.

of the instruments that have always played and will play a very important role on disaster managing, preparedness and intervention [4–6].

One example are social networks, they have been a distributed source of information with the ability to have local access to data in situ. Twitter and Facebook were used within the Ushahidi open-source crisis-mapping software in Haiti to gather information together with an SMS platform [7]. Also different technologies are being explored to provide first responders with enhanced communication capabilities to alleviate, resolve, or overcome an emergency situation. One of the key programs in 2016 for the US Department of Homeland Security was the usage of wearable technology that includes physiological sensors for health support, high-performance materials, communications capabilities, and context awareness.

1.1. Current and Future Public Safety and Emergency Networks. Narrowband Private Mobile Radio (PMR) systems support certain mission-critical features, i.e., device-to-device (D2D) calling, one-to-many calling, push-to-talk calling, etc. However enhanced capabilities such as robust broadband infrastructure, augmented information availability to enhance situational awareness, and rapidly deployable systems for streamline operations will rely on future wireless communication systems (LTE, LTE Advance-pro, 5G) [8] that, being aware of these advanced communications needs, are already proposing specific standardized solutions [9] for emergency scenarios.

New trends in business such as disruptive technologies, hypercompetition, new customer power and quality demands, etc. are affecting the vertical industries in different ways and this is why industries requirements are more and more demanding. Here is where 5G technologies, specifically network slicing, play a very relevant role. Traditionally, telecommunication networks were based on physical nodes that provided all the services that the operator offered and whose configuration was not performed automatically. Information and communications technologies (ICT) development have led to understand networks in a different way, introducing the concept of logical network, where networks are designed, instantiated, and operated on-demand, meeting

the requirements of the business, customers, or services. These logical networks are named network slices. A network slice, hence, covers a complete set of network functions to give a specific service. Therefore, network slices can tackle a huge variety of technical aspects to meet the requirements for each specific service. These requirements can go from latency, throughput (uplink and downlink), availability and resilience, reliability or coverage, to communication security aspects [10]. Public safety is one of the vertical industries whose requirements will be met with 5G technologies whose most important needs are a reliable connectivity, coverage, and enough throughput to transfer any content that may be helpful in a disaster situation.

In this work we explore two key aspects of public safety vertical: high-throughput and connectivity/coverage. With this aim, a network architecture based on relays for a rapidly deployable communication infrastructure is presented and spectral efficiency is improved by means of multiple-input-multiple-output (MIMO) antenna technology. MIMO technology here has a different approach which is targeting the user end by seamlessly deploying a large number of antennas in textile technology.

2. Technological Solution to Address Broadband Coverage

In this section we present a network architecture proposal for future public safety communications that may improve important weakness of current PMR networks such as the limited coverage and spectral efficiency giving rise to the use of multimedia services. The architecture envisions a two-hop relay network, merging massive MIMO textile technology into the LTE cellular network.

As depicted in Figure 1, in the proposed network three main components (base transceiver station (BTS), relay node, and user equipment (UE)) and two main links can be distinguished. One of them defines the base station coverage area which is defined between the base station and a relay node and the second one establishes the relay node coverage area between the repeater device and the user equipment.

2.1. Relay Node. Thanks to the Long Term Evolution-Advanced (LTE-A) standard defined by the 3GPP, different methods to improve coverage at relatively low cost to the operator have been brought in. Among them relay nodes can be highlighted.

Relay nodes are classified into different categories attending to different characteristics such as the level of the protocol stack in which the user traffic is transmitted, and the functions enabled in the control plane [11], and the transparency [12] with respect to the user or the use of the spectrum [13]. A more detailed explanation is given below.

2.1.1. Level in the Protocol Stack. Layer 1, 2, and 3 relay nodes can be distinguished in this category. Layer 1 relays (also known as repeaters) act amplifying and forwarding the downlink and uplink signals between the user equipment (UE) and the BTS, just like a simple analog amplifier. This fact allows extending the coverage area of an existing base station to locations where it cannot reach by itself. It should be noticed that Layer 1 relays work in a nontransparent mode and typically the noise from the link between the base station and the relay is amplified in the next link. Layer 2 and 3 relays essentially decode the incoming signal and remodulate and reencode it before the amplified version is forwarded. These kinds of relays avoid drawbacks such as noise being amplified and retransmitted.

2.1.2. Spectrum Use. Two types of relays can be distinguished depending on the use of the spectrum in the different links: in-band and out-of-band. In the first case, the link between the base station and the relay shares the same frequency as the link between the relay and the UE. On the other case, the link between the BTS and the relay does not share the same frequency as the link between the relay and the UE.

2.1.3. Transparency. The main difference between nontransparent and transparent operation modes lies in how framing information is transmitted. In nontransparent mode, the relay nodes transmit frame header information mainly containing scheduling information that it is useful for the nodes to know when they can transmit and receive information. Conversely, in transparent operation mode relay nodes do not transmit frame header information.

From now on, attending to the protocol stack classification we will assume an amplify-and-forward relay scenario.

2.2. Massive MIMO Textile Technology in the UE. To enable high spectral efficiency necessities of current public safety networks, the textile antenna technology, which allows us to deploy MIMO-based personal area networks in the proximity of the human body, appears to be a promising solution [14]. The main idea behind this technology consists on embedding a large textile antenna array which acts as a transmitter/receiver at the user's garments (see Figure 2), bringing the benefits of massive MIMO directly to the user's end. It must



FIGURE 2: Real large textile antenna array deployed at user jacket backside.

TABLE 1: Design features of the large textile antenna using CST Microwave Studio.

Working Frequency	2.5 GHz
Planar array Size	8×5
Inter-element distance (avoiding Mutual Coupling)	0.66λ
Dielectric Substrate	Common Felt ($\epsilon_r = 1.38$)
Metallization	Electrotextile Material
Array Area	$44.6 \times 60.6 \text{ cm}^2$
Backward power levels	-20 dB
Bandwidth	70 MHz

be noticed that communications using the textile technology may be on-body (wireless communication link between devices placed in the body of the user) or off-body (wireless link is established between devices placed in the body such as a video camera and an external element like the base station).

We consider a textile planar array whose main features are described in [14, 15] and summarized in Table 1. The number of antennas of this particular design is $N = 40$; nevertheless other configurations will also be explored in Section 4.

3. MIMO-Relaying Scenario Modeling and Performance

We analyze a two-hop single relay scenario with multiple radiating elements at the source/BTS (M), relay (R), and destination/UE (N) working in an amplify-and-forward mode (Layer 1 relay). The relay node is assumed to work in half-duplex mode. This means that communication from source to relay and from relay to destination is carried out in two different time slots. Additionally, we assume that there is no direct link between the source and destination.

During the first time slot, the transmitted signal from the source propagates through the first-hop channel, and the received signal at the relay is given by

$$\mathbf{y}_r = \sqrt{\rho_r} \mathbf{H}_{sr} \mathbf{x}_s + \mathbf{n}_r \quad (1)$$

where \mathbf{x}_s is the $M \times 1$ transmitted signal vector with normalized power, \mathbf{H}_{sr} is the $R \times M$ channel matrix between the source and the relay, ρ_r is the signal-to-noise ratio (SNR) of the source-relay link, and \mathbf{n}_r is the $R \times 1$ relay noise vector with normalized variance.

During the second time slot, the relay amplifies the received signal defined in (1) and forwards it to the destination. The received signal at the UE is as follows:

$$\mathbf{y}_d = \sqrt{\rho_d} \mathbf{H}_{rd} \mathbf{G} \mathbf{H}_{sr} \mathbf{x}_s + [\sqrt{\rho_d} \mathbf{H}_{rd} \mathbf{G} \mathbf{I}] \begin{bmatrix} \mathbf{n}_r \\ \mathbf{n}_d \end{bmatrix} \quad (2)$$

where \mathbf{H}_{rd} is the $N \times R$ channel matrix between the relay and the destination, \mathbf{G} is the $R \times R$ relay amplification factor, ρ_d is the relay-destination link SNR, and \mathbf{n}_r is the $N \times 1$ destination noise vector with normalized variance.

3.1. Channel Model. In our analysis, the first-hop channel \mathbf{H}_{sr} is modeled by a Rayleigh i.i.d. fading distribution, assuming a full-scattering environment and large spacing among antennas at both, the BTS and the relay. The second hop channel \mathbf{H}_{rd} , defined between the UE equipped with MIMO textile technology and the relay node, is modeled to take into account the textile antenna parameters and radiation patterns in transmission and reception and the surrounding scattering environment. Each element h_{mm} in the channel matrix \mathbf{H}_{rd} is described by the Green's function sampled at the position of the n -th receiving antenna \mathbf{r}'_n given that the point source is located at the m -th transmitting antenna (\mathbf{r}_m) [16]:

$$h_{mm} = \iint \mathcal{E}_m(\theta, \phi) \mathcal{E}'_n(\theta', \phi') S(\mathbf{k}'(\theta', \phi'), \mathbf{k}(\theta, \phi)) \cdot e^{-j\mathbf{k}(\theta, \phi) \cdot \mathbf{r}_m} e^{j\mathbf{k}'(\theta', \phi') \cdot \mathbf{r}'_n} d\mathbf{k}'(\theta', \phi') d\mathbf{k}(\theta, \phi) \quad (3)$$

where $\mathcal{E}_m(\theta, \phi)$ and $\mathcal{E}'_n(\theta', \phi')$ represent the radiation patterns in azimuth (ϕ) and elevation (θ) at the transmitter and receiver, respectively, $\mathbf{k}(\theta, \phi)$ and $\mathbf{k}'(\theta', \phi')$ are the wave vector space at the transmitter and receiver, respectively, and $S(\mathbf{k}'(\theta', \phi'), \mathbf{k}(\theta, \phi))$ is the channel scattering function, which relates the plane wave's emitting and receiving directions, \mathbf{k} and \mathbf{k}' , respectively. It must be noticed that this channel model assumes single-polarized antennas as the ones described in Section 2.2 and therefore the transmit and receive vector fields together with the channel scattering function can be considered scalars. However, this model could be easily extended to further consider different polarization if we work with vectorial fields and a dyad transformation function as scattering [17, 18].

The vector space can be sampled into L plane waves at the transmitter and L' plane waves at the receiver to cover the

entire space. Then, the channel matrix can be decomposed [19] into the product of five matrices $\mathbf{H}_{rd} = \mathbf{B}_{rx}^\dagger \Sigma_{rx} \mathbf{H}_{iid} \Sigma_{tx} \mathbf{B}_{tx}$, where \mathbf{B}_{rx} ($L' \times N$) and \mathbf{B}_{tx} ($L \times R$) are beamforming matrices depending on the antenna geometry and radiation patterns, \mathbf{H}_{iid} ($L' \times L$) is a complex Gaussian random matrix with i.i.d. components and variance one, and Σ_{rx} and Σ_{tx} are normalized diagonal matrices whose main diagonal is shaped with the corresponding angular power spectra. The MC between antenna elements is then captured via the coupling matrices \mathbf{C}_{tx} and \mathbf{C}_{rx} as shown in [12]. The resulting channel matrix is given by $\mathbf{H}_{rd} = \mathbf{C}_{rx} \mathbf{B}_{rx}^\dagger \Sigma_{rx}^{1/2} \mathbf{G} \Sigma_{tx}^{1/2} \mathbf{B}_{tx} \mathbf{C}_{tx}$.

3.2. Relay Amplification Factor. We assume that the relay node simply applies a linear transformation on the received signal \mathbf{y}_r by means of the relay amplification factor \mathbf{G} as follows:

$$\mathbf{G} = \beta \mathbf{I}_R \quad (4)$$

Parameter β is defined in order to achieve the relay-destination link SNR ρ_d [20, 21]:

$$\beta = \sqrt{\frac{1}{\rho_r \|\mathbf{H}_{sr}\|_F^2 + 1}} \quad (5)$$

where $\|\cdot\|_F^2$ represents the squared Frobenius norm. It must be noticed that in our model the power is assumed to be allocated uniformly over all the antennas.

3.3. Achievable Rates for the Relay Scenario. The achievable rates of the amplify-and-forward half-duplex MIMO-based two-hop single relay channel with \mathbf{G} as in (4) and (5) can be written as in (6) [22, 23].

Since the transmission is completed in two different time instances, the spectral efficiency is reduced by half and the SNR of each of the links are doubled.

4. Results and Discussion

In this section, we evaluate the performance of the two-hop relay architecture in terms of achievable rates with different antenna configurations. On the one hand, we analyze the achieved capacity in one scenario where the textile array deployed at the UE is built with $N = 40$ antennas and the BTS and relay count with $M = R = \{1, 4, 8, 20\}$. On the other hand, we analyze the optimal relay position to maximize the achieved capacity for different antenna configurations. In this particular case, we consider the same number of antennas in all communications ends $M = R = N = \{1, 2, 4, 6, 10\}$ and study the impact of the SNR level on the optimization. Simulations are carried out generating 500 channel samples using the channel model presented in Section 3.

Figure 3 shows the achieved capacity when different levels of SNR. At low SNR values such as SNR = 0 dB data rates values from approximately 1.6 Mbps up to 48 Mbps can be achieved considering a bandwidth of 10 MHz. On the other hand, at high SNR regimes like SNR = 10 dB, achieved data rates go from 10 Mbps up to 200 Mbps. As expected, the achieved capacity increases as the number of antennas increases.

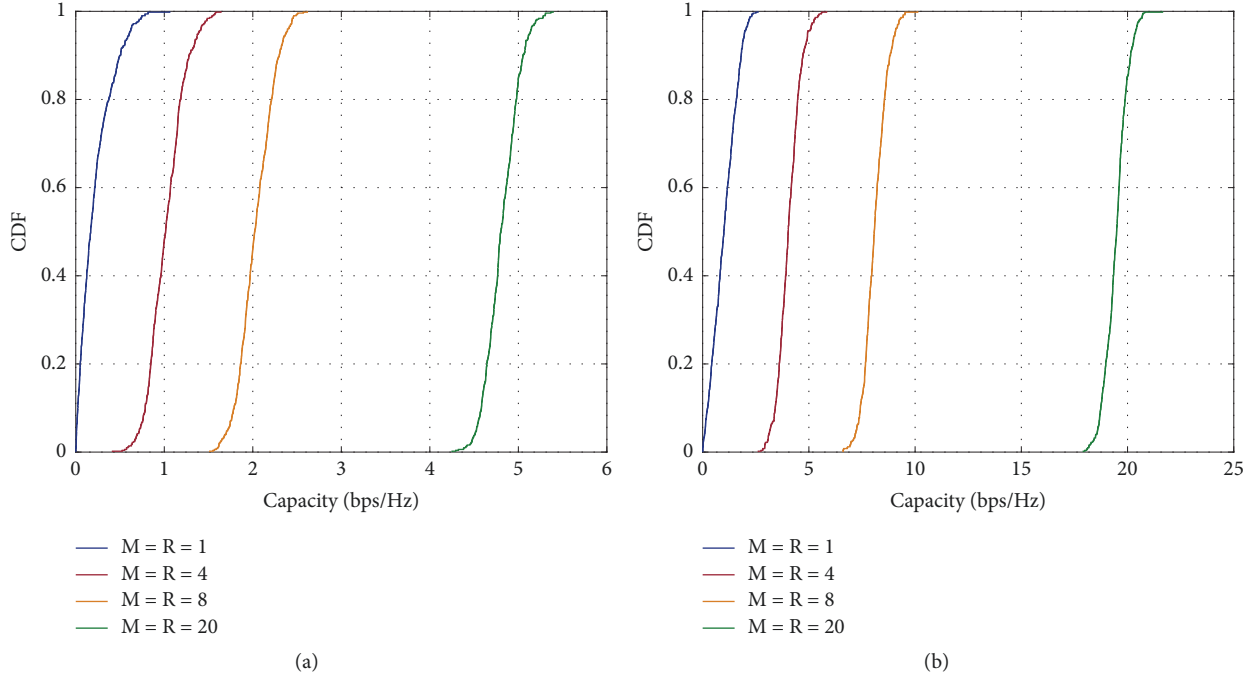


FIGURE 3: Achievable rates with different antenna configurations (a) achieved rates for $N = 40$, $R = M = \{1, 4, 8, 20\}$, and $\text{SNR}(\text{dB}) = 0$; (b) achieved rates for $N = 40$, $M = R = \{1, 4, 8, 20\}$, and $\text{SNR}(\text{dB}) = 10$.

4.1. Optimal Relay Allocation. Scenarios with low SNR are the candidates for the deployment of a MIMO-based relay solution to increase coverage or improve rates. To illustrate that, we will show next the average achievable rates in different positions of the relay. The SNR model assumes an exponent path loss of 3.32 which has been measured in outdoor-to-indoor scenarios with the UE equipped with textile antennas placed underground [24]. The plots include as a reference the achievable rates of a direct link scenario, with no relay, showing which is the best relay configuration (normalized position) to improve the direct link achievable rates.

$$R = \frac{1}{2} \log_2 \det \left(\mathbf{I}_N + \frac{4\rho_d\rho_r}{M} \frac{\mathbf{H}_{rd}\mathbf{H}_{sr}\mathbf{H}_{sr}^\dagger\mathbf{H}_{rd}^\dagger}{2\rho_d\mathbf{H}_{rd}\mathbf{H}_{rd}^\dagger + 2\rho_r\|\mathbf{H}_{sr}\|_F^2\mathbf{I}_N + \mathbf{I}_N} \right) \quad (6)$$

From Figure 4 it is possible to corroborate that the relay node presence appears to be especially useful at low SNR scenarios. In fact, as the SNR value increases, the performance of the relay network in terms of capacity falls slightly below the direct link case. Depending on the existing number of antennas, the coverage region where the relay node is useful (relay capacity is higher than the direct link capacity) varies, being smaller as the number of antennas increases. Furthermore, from the results in Figure 4 we can also obtain the optimal relay position leading to the maximum achievable rate in those scenarios where

the relay architecture outperforms the direct link transmission.

5. Conclusions

This work proposes a network and physical layer solution based on LTE-A and future 5G capabilities to improve public safety communications, which are currently conveyed through narrowband PMR systems and mainly focused on offering limited voice services. We have analyzed the performance in terms of capacity of an amplify-and-forward relay network when massive MIMO textile technology is deployed at the user side. Additionally, we have evaluated the optimal relay location with the purpose of maximizing the achieved capacity in the two-hop network. Simulation results illustrate the viability of the proposed design, specifically for low SNR scenarios where the relay node will allow us to extend the coverage and the MIMO textile technology to improve the capacity.

Data Availability

We have no included a data availability statement in our article.

Conflicts of Interest

The authors declare that there are no conflicts of interest regarding the publication of this paper.

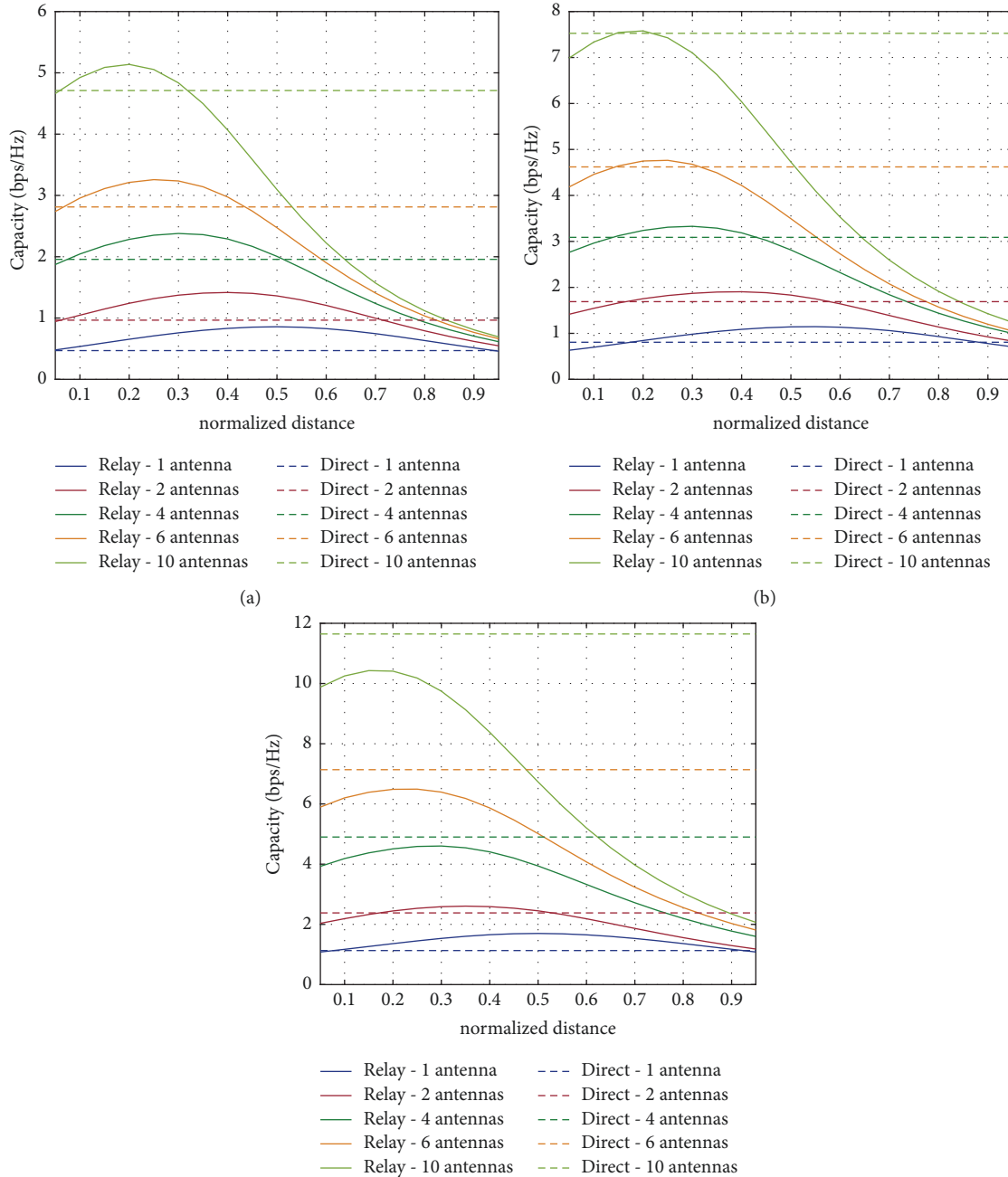


FIGURE 4: Relation between the normalized relay location and the achieved capacity at different SNR regimes and antenna configurations, considering $M = R = N$. (a) $SNR = -3$ dB; (b) $SNR = 0$ dB; and (c) $SNR = 3$ dB.

Acknowledgments

This work has been partly funded by the Spanish Government through Projects CIES (RTC-2015-4213-7), MIMO-TEX (TEC2014-61776-EXP), and TERESA-ADA (TEC2017-90093-C3-2-R) (MINECO/AEI/FEDER, UE).

References

- [1] D. Sanderson and A. Sharma, *World Disasters Report, Resilience: Saving Lives Today, Investing for Tomorrow*, International Federation of Red Cross and Red Crescent Societies, 2016.
- [2] D. Guha-Sapir and R. Below, "Collecting data on disasters: easier said than done," *Asian Disaster Management News*, vol. 12, no. 2, pp. 9-10, 2006.
- [3] United Nations Office for Disaster Risk Reduction, "Sendai framework for disaster risk reduction 2015 - 2030," Tech. Rep., Sendai, Japan, 2015, https://www.preventionweb.net/files/43291_sendaiframeworkfordrren.pdf.
- [4] I. Kamen, "A new approach to disaster communication and control systems," *Electrical Engineering*, vol. 81, pp. 535-541, 1962.
- [5] T. C. Chan, J. Killeen, W. Griswold, and L. Lenert, "Information technology and emergency medical care during disasters," *Academic Emergency Medicine*, vol. 11, no. 11, pp. 1229-1236, 2004.

- [6] R. Shaw, T. Izumi, and P. Shi, "Perspectives of science and technology in disaster risk reduction of asia," *International Journal of Disaster Risk Science*, vol. 7, no. 4, pp. 329–342, 2016.
- [7] J. Heinzelman and C. Waters, "Crowdsourcing crisis information in disaster-affected Haiti," Tech. Rep., United States Institute of Peace, 2010.
- [8] T. Doumi, M. F. Dolan, S. Tatesh et al., "LTE for public safety networks," *IEEE Communications Magazine*, vol. 51, no. 2, pp. 106–112, 2013.
- [9] 3GPP, "Isolated evolved universal terrestrial radio access network (E-UTRAN) operation for public safety, stage 1," Tech. Rep. TS 22.346, Release 13, 2014.
- [10] GSA, *5G network slicing for vertical industries*, GSA White Paper, 2017.
- [11] M. Iwamura, H. Takahashi, and S. Nagata, "Relay technology in LTE-advanced," *NTT DoCoMo Technical Journal*, vol. 12, no. 2, pp. 29–36, 2010.
- [12] H. Holma and A. Toskala, *LTE advanced: 3GPP solution for IMT-Advanced*, John Wiley and Sons, 2012.
- [13] 3GPP, "Feasibility study for further advancements for E-UTRA (LTE-advanced)," Tech. Rep. G. TR 36.912, 2012.
- [14] M. Sanchez-Fernandez, A. Tulino, E. Rajo-Iglesias, J. Llorca, and A. G. Armada, "Blended antenna wearables for an unconstrained mobile experience," *IEEE Communications Magazine*, vol. 55, no. 4, pp. 160–168, 2017.
- [15] E. Crespo-Bardera, M. Sánchez-Fernández, A. García-Armada, A. G. Martín, and A. F. Durán, "Analysis of a LTE-based textile massive MIMO proposal for public safety networks," in *Proceedings of the 86th IEEE Vehicular Technology Conference, VTC Fall '17*, pp. 1–5, September 2017.
- [16] D. Chizhik, "Slowing the time-fluctuating MIMO channel by beam forming," *IEEE Transactions on Wireless Communications*, vol. 3, no. 5, pp. 1554–1565, 2004.
- [17] T. Svantesson, "A physical MIMO radio channel model for multi-element multi-polarized antenna systems," in *Proceedings of the IEEE 54th Vehicular Technology Conference, VTC Fall '01*, vol. 2, pp. 1083–1087, IEEE, October 2001.
- [18] M. L. Pablo-González, M. Sánchez-Fernández, and E. Rajo-Iglesias, "Combination of the three types of diversity to design high-capacity compact MIMO terminals," *IEEE Antennas and Wireless Propagation Letters*, vol. 13, pp. 1309–1312, 2014.
- [19] P. N. Fletcher, M. Dean, and A. R. Nix, "Mutual coupling in multi-element array antennas and its influence on MIMO channel capacity," *IEEE Electronics Letters*, vol. 39, no. 4, pp. 342–344, 2003.
- [20] L. Jiang, L. Thiele, and V. Jungnickel, "Modeling and measurement of MIMO relay channels," in *Proceedings of the IEEE 67th Vehicular Technology Conference-Spring, VTC '08*, pp. 419–423, IEEE, May 2008.
- [21] T. Q. Duong, L.-N. Hoang, and V. N. Q. Bao, "On the performance of two-way amplify-and-forward relay networks," *IEICE Transactions on Communications*, vol. E92-B, no. 12, pp. 3957–3959, 2009.
- [22] P. Herhold, E. Zimmermann, and G. Fettweis, "On the performance of cooperative amplify-and-forward relay networks," *ITG FACHBERICHT*, vol. 2, pp. 451–458, 2004.
- [23] M. Herdin, "MIMO amplify-and-forward relaying in correlated MIMO channels," in *Proceedings of the 5th International Conference on Information, Communications and Signal Processing*, pp. 796–800, IEEE, 2005.
- [24] E. Crespo-Bardera, M. Rodríguez, M. Sánchez-Fernández et al., "Empirical rates characterization of wearable multi-antenna terminals for first-responders," *IEEE Access*, vol. 7, pp. 6990–7000, 2019.



Hindawi

Submit your manuscripts at
www.hindawi.com

